

CIRP Conference on Electro Physical and Chemical Machining 2019

Development of Process Chain for Micro-Injection Molding

Büttner, H.^{a*}, Maradia, U.^b, Suarez, M.^c, Stirnimann, J.^a, Wegener, K.^a

^a*Institute of Machine Tools and Manufacturing, ETH Zürich, Switzerland*

^b*GF Machining Solutions, Losone, Switzerland*

^c*Institute of Materials Technology and Plastics Processing, HS Rapperswil, Switzerland*

* H. Büttner. Tel.: +41 44 632 54 84; fax: +41 44 632 11 25. E-mail address: buettner@inspire.ethz.ch

Abstract

In today's continuously growing demand for components with increasingly smaller dimensions and features, micro-manufacturing is gaining more significance. For the mass production of plastic components with micro-features, injection molding is particularly suitable and still customary in order to keep target costs. Due to high requirements regarding lifetime and resistance to wear, the molds are made of hardened steel. The shaping of these molds involves electrical discharge machining (EDM). This process allows the generation of micro-structures in micrometer range having small inner radii, high dimensional accuracy and extreme aspect ratio independent of the workpiece hardness. As a work tool for EDM, electrodes made of pure copper (Cu) and tungsten reinforced copper (WCu) are commonly used. The shaping of the electrodes is conducted by micro-milling. For an overall understanding of this process chain, the interaction between micro-milling, micro-EDM, and micro-injection molding must be evaluated. This paper provides knowledge on the limits of each process with regard to burr formation, form accuracy, structure size and aspect ratio. Many factors throughout the process chain affect the size of an attainable micro-feature of a final product. The proper selection of the electrode material is a key factor in the process chain. As the feature size of the electrode defines the dimension of the final product shape, the smallest possible structures have to be found during micro-milling. The dimension of the eroded cavity is defined by the feature size of the electrode in combination with the lateral working gap. Eroded cavities with small inner corner radii and steep flanks can be generated when applying flawless and burr-free electrodes. However, using electrodes in inadequate conditions can lead to worse outcomes. The quality and reliability of the final product are determined to a great extent by the design of the injection molding process. Due to the arising vacuum when evacuating the remaining air in the mold, the inflowing melt is being distributed equally. It must be guaranteed that during injection molding, the mold is thermally-controlled. This prevents premature solidification. Through a combination of these two strategies, a form filling rate in micro-cavities up to 100 % is carried out. By deriving an impeccably adapted process chain, a precise micro-molding can be performed. This leads to the capability of manufacturing bars on a final plastic part with a width and height as low as 55 x 100 µm, and a length of 2 mm.

© 2019 The Authors. Published by Elsevier Ltd. This is an open access article under the CC BY-NC-ND license (<http://creativecommons.org/licenses/by-nc-nd/3.0/>)

Peer-review under responsibility of the scientific committee of the 20th CIRP Conference on Electro Physical and Chemical Machining.

Keywords: micro-machining; micro-milling; micro-die-sinking EDM; micro-injection molding

1. Introduction

The ability to machine microstructures is desirable for many applications ranging from miniaturization to func-

tionalization of large surfaces. However, the manufacturing of polymer parts with micro-features involves not only micro-injection molding but also technologies for mold shaping. In this regard, the desired structure sizes and the

2212-8271 © 2019 The Authors. Published by Elsevier Ltd. This is an open access article under the CC BY-NC-ND license (<http://creativecommons.org/licenses/by-nc-nd/3.0/>)

Peer-review under responsibility of the scientific committee of the 52nd CIRP Conference on Manufacturing Systems.

necessary tolerances of a mold have to be considered. These requirements address different technologies for mold manufacturing. P. Roy [17] and G. L. Benavides et al. [2] present the capability of LIGA-machining, which is feasible to manufacture structure dimensions ranging from 0.1...500 μm with tolerances as low as 0.02 μm . Besides the capability of manufacturing features with small dimensions, LIGA is limited to 2.5-D shaping. Also, it does not apply to machine tool steel. As an alternative, Benavides et al. [2] suggest mold shaping using laser-beam machining (LBM). This process is limited due to the laser spot size and a relatively high surface roughness.

According to Zhao et al. [21], EDM is a suitable technology for mold shaping. It allows the formation of structure size smaller than $< 20 \mu\text{m}$ with low tolerance deviations, independent on the workpiece hardness. Büttner et al. [3] investigate the behavior of Cu during wire-EDM machining. With optimized parameters flawless micro-bars having a width $W_B = 70 \mu\text{m}$, a height $H_B = 350 \mu\text{m}$, and a pitch $P_B = 320 \mu\text{m}$ are feasible to machine using a wire with a diameter D_W as low as $\varnothing = 200 \mu\text{m}$.

With the aim to minimize structure dimensions, micro-die-sinking EDM using copper (Cu) and tungsten reinforced copper (WCu) electrodes is performed to generate micro-cavities in 1.2344 steel. For this purpose, the limits of micro-structuring the electrodes using micro-milling is first investigated and secondly, the limits of micro-die-sinking EDM are analyzed. It is seen, that the dimensions of the employed milling-tool and the lateral working gap G primary limit an achievable structure density. Also, the mechanical properties of Cu and WCu lead to bending of structures when increasing the aspect ratio AR , as the stiffness k decreases. With the constraint of a minimal working gap G together with minimal electrode structure sizes, the usual strategy applying roughing- and finishing- technologies in EDM is not possible. Due to the higher discharge energy W_E , a larger working gap G has to be expected, which causes an enlargement of the dimensions of the micro-cavities in the mold.

As pointed out by Giboz et al. [6], conventional injection molding differs strongly from micro-injection molding. The main aspect mentioned addresses mold heating. Mendoza [15] observes a material property variation along with the thickness of the melt caused by different cooling conditions during the process. These variations influence the mechanical properties of the final part. In concordance, Gornik [8] describes the impact of process conditions on the quality of replicated parts. Due to the higher volume to surface ratio, the cooling rate of the melt in the case of micro-injection molding is more pronounced compared to conventional molding, as mentioned by Whiteside et al. [19]. Premature solidification of the melt during the process favors the formation of defects in the final part. Thus, heating of the mold is recommended for maintaining flawless structures. Gornik [8] describes the advantage of a variotherm process. Additionally, Yao [20] presents the performance of the variotherm process, when micro-structures with high aspect ratios AR are required. This strategy prevents material degradation due to shrinking. Besides, the residual stresses can be minimized, as the cooling phase is adjusted, as discussed by Chen et al. [4]. The importance of the mold temperature is stated by Hecke

and Schomburg [9], Schiff et al. [18] and McFarland et al. [14]. To guarantee a high form filling ratio R , the mold temperature must be located in the range of the softening temperature of the polymer. D'Amore et al. [5] correlate the temperature with the aspect ratio AR of a micro-structure. For a higher ratio, the temperature must adopt higher values. Also, a high temperature allows a reduction of injection pressure and injection speed. A presence of air in the cavity causes a low tolerance of the final part and thus must be evacuated.

Summarizing, an accordingly adjusted process chain has to be derived, when the manufacturing of a plastic part with micro-features is required. The final product quality is dependent on a great extent on the condition of the mold and the design of the micro-injection molding process. Minimal feature sizes on the final part are determined already in the first stage of the process chain. Hence, electrode and mold shaping are crucial and require small feature sizes, high form accuracy, prevention of burr formation, and so on. It is seen that the mold temperature has a major impact, thus mold heating using variotherm has to be applied. Also, the proper choice of polymer type must be evaluated.

2. Tool Preparation

2.1 Micro-Milling

For minimizing the micro-structures on a final plastic part, the minimal achievable structure sizes on the electrodes have to be found. Besides the miniaturization, also high requirements on the quality of the micro-structure are placed. Beside other factors, the following aspects have to be addressed during micro-milling of micro-structures:

- Preventing burr formation.
- Ensuring sharp edge radii r_{edge} .
- Consideration of milling direction.
- Optimizing of process parameters and conditions.
- Form accuracy and high flank steepness.
- Mechanical properties of the workpiece.

The micro-milling experiments are conducted on a 5-axis-machining center of the type HSM 200 U LP from Georg Fischer Machining Solutions (GFMS), Switzerland. A Levicron spindle provides a rotation speed as high as $n_{\text{max}} = 90.000 \text{ rpm}$. The experiments are supported by a minimum quantity lubrication (MQL) system. Tool diameter and length are detected by an M&H laser micrometer bridge, which allows the measurement of tools with a diameter as low as $\varnothing = 25 \mu\text{m}$ with a measurement uncertainty of $\pm 0.2 \mu\text{m}$.

The employed electrodes are made of pure Cu (99% Cu) and WCu (75% W and 25% Cu), as these materials exhibit high electrical and thermal conductivity. However, the materials differ strongly from hardness and strength. Therefore, a disparate material response during machining has to be expected. Micro-tools made of tungsten carbide (WC) with two cutting edges are employed for investigations. The tools have a diameter as low as $\varnothing = 150 \mu\text{m}$ and a cutting edge length as low as $l_{\text{cut}} = 300 \mu\text{m}$.

Burr-free and sharp-edge machining

The formation of burrs during micro-milling must be prevented, high flank steepness guaranteed, bending of the micro-structures avoided, and small edge radii ensured. To

achieve these requirements, it is essential to optimize the micro-milling strategy. This includes the proper choice of process parameters, tool path planning, and selection of a reasonable milling direction.

When performing micro-milling without tool path optimization, different types of burr formation are observed. According to Gillespie and Blotter [7] and Reichenbach et al. [16], the basic types of burr are defined as: Poisson burr, roll-over burr, tear burr, and cut-off burr. When machining bars, these burrs occur in four different regions and are classified to: entrance burr (I), exit burr (II), and top burr (III), as shown in Figure 1 a). Also, burr formation on the flank face (IV) of the micro-structure is observed due to ploughing of material. Burr-formation is avoided when conduction micro-milling using burr-free strategy, as shown in Figure 1 b).

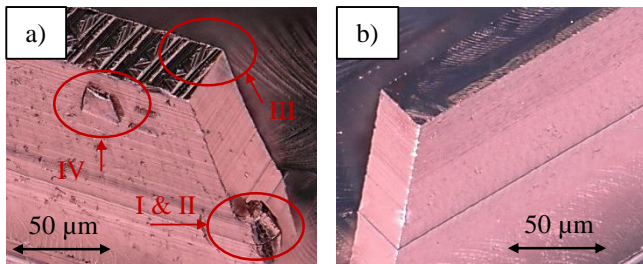


Figure 1 Burr formation when micro-milling Cu; a) observation of four burr types; b) burr-free micro-structure.

The burr-free micro-milling strategy comprises three sequential steps, as shown in Figure 2. Initially, the machining is performed until the desired dimension is reached, as displayed in Figure 2 a). The tool is fed into the material with a width a_c and depth a_p of cut. In this step, special attention must be given to the edge sharpness of the micro-structures. It is important that the tool exits an edge in a loop-trajectory with a defined radius r_{loop} and engages the edge tangentially in the direction of the subsequent path. Doing so allows the formation of sharp edge radii r_{edge} . The loop radius r_{loop} must be chosen in accordance with the deceleration and acceleration distance of the machine drives. As the final dimension is reached, the tool is guided around the micro-structure without lateral infeed having a width of cut $a_c = 0 \mu\text{m}$, as shown in Figure 2 b). This allows the subsequent removal of lateral burrs.

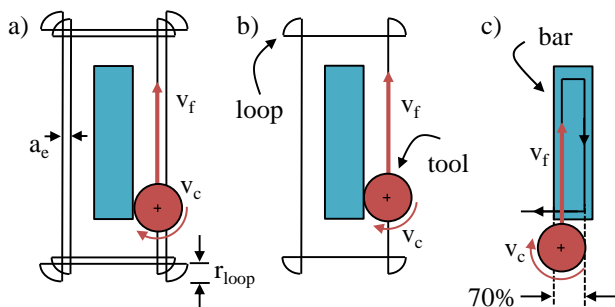


Figure 2 Milling Strategy for burr-free machining; a) roughing to achieve final dimension; b) deburring of lateral burrs; c) deburring of top burrs.

During the concluding step, the tool moves along the top surface without infeed in the vertical direction having a depth of cut $a_p = 0 \mu\text{m}$. This step has to be performed in the

up-milling direction, to bend an occurring burr in the direction of the structure and thus, guaranteeing material shearing. Also, the tool overlaps the surface 70% of the structure width, as shown in Figure 2 c).

Milling direction

Besides the optimization of tool path planning, also the direction of cutting must be evaluated. As described by Heisel et al. [10] and Llanos et al. [13], up-milling leads to a higher surface quality compared to down-milling. However, Li et al. [12] mention, that a high fluctuation of process forces when up-milling adversely influences the form accuracy. In concordance, Annoni et al. [1], Kiswanto et al. [11] and Li et al. [12] discuss the process force reduction when performing down-milling.

For micro-milling Cu and WCu a similar behavior is observed. When performing up-milling, surface defects at the bottom of the flanks are pronounced. Figure 3 displays the impact of the milling direction when machining WCu. The imaging position is indicated in Figure 6 with the marker (I). Due to ploughing effects, the material is not completely removed, but rather plastically deformed when performing up-milling, as shown in Figure 3 a). A sharp transition of the flank to the base is feasible when performing down-milling, as seen in Figure 3 b).

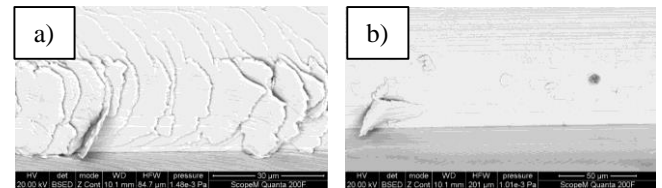


Figure 3 Impact of milling direction when machining WCu; a) surface defects in up-milling; b) enhance of surface quality in down-milling.

Process parameters

A further improvement of micro-structure quality is feasible when choosing proper process parameters. The spindle speed $n_{max} = 90.000 \text{ rpm}$ provides a cutting speed $v_c = 42 \text{ m/min}$ for tools having a diameter $\varnothing = 150 \mu\text{m}$. The width of cut is as low as $a_c = 30 \mu\text{m}$. However, it is found that the depth of cut a_p exhibits the main impact on the resultant quality, as the z-levels are pronounced on the flanks. As a consequence, the depth of cut is reduced down to $a_p = 5 \mu\text{m}$. To increase productivity, it is observed that the feed rate can be increased from $v_f = 540 \text{ mm/min}$ up to $v_f = 1800 \text{ mm/min}$, without affecting the quality.

Achievable dimensions

With an increase in the aspect ratio AR of the micro-structures, a reduction of the stiffness k has to be expected. This causes bending, deformation and favors the appearance of conical flanks. To determine the maximal achievable aspect ratio AR, micro-structures in Cu and WCu are generated. The height is held constant and is set as high as $H_B = 290 \mu\text{m}$, as the cutting edge length of the tool is $l_{cut} = 300 \mu\text{m}$. Also, the distance between two bars is held constant to $D_B = 190 \mu\text{m}$. The width of the bars is reduced from $W_{Bar} = 60 \dots 30 \mu\text{m}$. These values correspond to aspect ratios ranging from $AR = 5 \dots 10$. Figure 4 displays the bars when micro-milling Cu. Flawless and burr-free bars with a

form accuracy below $5\ \mu\text{m}$ and an aspect ratio of $AR = 5$ are feasible to machine, as seen in Figure 4 a) & b). A further increase of the aspect ratio to $AR = 5$ and 7 causes a form deviation of $\sim 7\ \mu\text{m}$, as shown in Figure 4 c) – f). Having an aspect ratio up to $AR = 10$ leads to a pronounced conical shape of the flanks, according to Figure 4 g) and h).

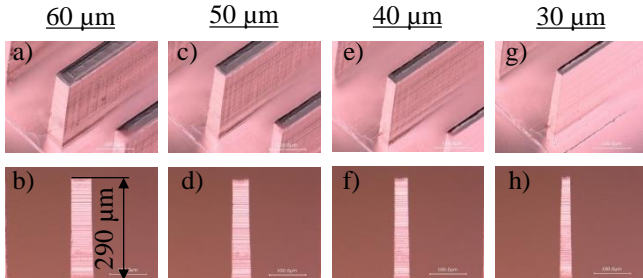


Figure 4 Burr-free bars in Cu with high aspect ratio AR ; a) & b) flawless bars having an $AR = 5$; c) – f) deviation from width of $\sim 7\ \mu\text{m}$; g) & h) conical shape pronounced.

When machining WCu a similar behavior is observed, as shown in Figure 5. According to Figure 5 a) & b), flawless bars in WCu with an aspect ratio $AR = 5$ are feasible to machine. However, unlike Cu, an increase of the aspect ratio leads to a bending of the bar, as shown in Figure 5 c) – f). Having an aspect ratio up to $AR = 10$ leads to a pronounced conical shape of the bar, according to Figure 5 g) and h). It can be concluded, that aspect ratio for Cu and WCu as high as $AR = 6$ are feasible to machine without damaging the micro-structure.

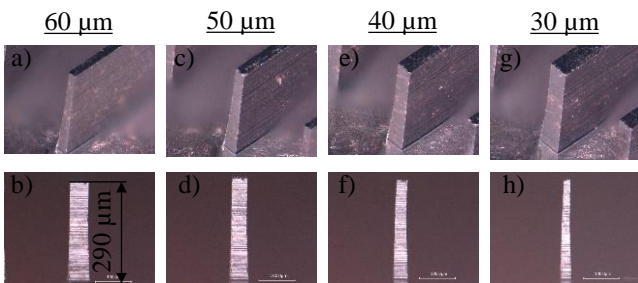


Figure 5 Burr-free bars in WCu with high aspect ratio AR ; a) & b) flawless bars having an $AR = 5$; c) – f) deviation from width of $\sim 7\ \mu\text{m}$; g) & h) conical shape pronounced.

The edge radii r_{edge} of bars in Cu and WCu are measured using an optical microscope of the type Alicona InfiniteFocus, as shown in Figure 6. The radii are analyzed on two regions and categorized as inner radius r_{inner} (as highlighted in green) and outer radius r_{outer} (as highlighted in red). It is observed, that both radii differ from each other, as the shape of the tool is replicated along the inner radii r_{inner} . This results in a higher value when compared to the outer radii r_{outer} . However, the inner radius r_{inner} can be neglected, as in subsequent die-sinking EDM this area is not in interaction with the workpiece. The outer radius r_{outer} adopts similar values for both materials. As WCu is a sintered material, edge defects occur due to partial break out of individual grains, which is indicated using an arrow at measuring position 3. This results in an enlargement of the outer radii r_{outer} and a higher standard deviation in comparison to Cu. In contrast, the edge quality for Cu is presented at measuring position 7.

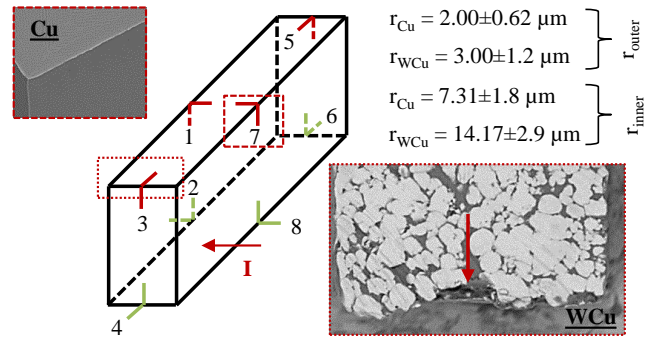


Figure 6 Representation of edge measuring locations.

2.2 Micro-die-sinking EDM

As the mold is made of hardened 1.2344 steel, the shaping technologies are limited for economically reliable machining. Also, the need for small cavity radii r_{cav} , low surface roughness R_a and high requirements on flank steepness further narrow the possibilities.

The shaping of the mold is performed using die-sinking EDM applying the micro-structured Cu and WCu electrodes. Die-sinking EDM is highly affected by electrode tool wear. Hence, the wear is compensated due to polarity, optimization of process parameters and the use of multiple electrodes for one shape in the workpiece.

Figure 7 displays a workpiece made of 1.2344 steel having micro-cavities. It is machined by micro-die sinking EDM using the Cu electrodes. Having frontal wear as low as $5\ \mu\text{m}$ and lateral wear below $2\ \mu\text{m}$, merely one Cu electrode for roughing and one for finishing are necessary. The electrodes employed exhibit 5 flawless and burr-free bars with each a width $W_{\text{Bar}} = 50\ \mu\text{m}$, height $H_{\text{Bar}} = 290\ \mu\text{m}$ and pitch $P_{\text{Bar}} = 250\ \mu\text{m}$. According to Figure 7 a), a non-measurable burr is formed during erosion. In Figure 7 b), a conicity smaller than $2\ \mu\text{m}$ along a depth of the cavity $D_{\text{cav}} = 150\ \mu\text{m}$ is seen. A high form accuracy is guaranteed. Also, as the working gap is below $G < 5\ \mu\text{m}$, the resultant width of the cavity is as low as $W_{\text{cav}} = 55\ \mu\text{m}$. Figure 7 c) and d) show, that a corner radius as small as $r_{\text{cav}} < 7\ \mu\text{m}$ is feasible to machine. The dimension of the corner cavity radius r_{cav} results as a combination of the outer radii on the Cu electrode of $r_{\text{outer,Cu}} = 2.00 \pm 0.62\ \mu\text{m}$ and the working gap on one side $G = 2.5\ \mu\text{m}$.

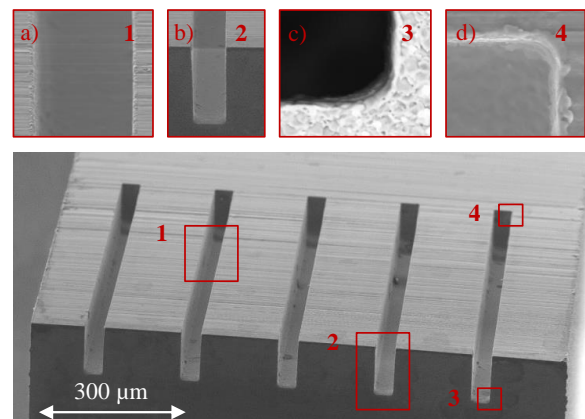


Figure 7 Workpiece eroded using 2 Cu electrodes.

The shape quality of the eroded workpiece is further improved by using 5 WCu electrodes, as shown in Figure 8. The width of a cavity is as low as $W_{cav} = 55 \mu\text{m}$, the depth as low as $D_{cav} = 150 \mu\text{m}$ and the pitch as low as $P_{cav} = 250 \mu\text{m}$. According to Figure 8 a) and b), the burr-formation is negligible and the conicity smaller than $2 \mu\text{m}$. By having a working gap as low as $G = 5 \mu\text{m}$, a corner cavity radius smaller than $r_{cav} < 3 \mu\text{m}$ is feasible to machine.

As a consequence, it can be derived that the shape of the eroded cavity is primarily dependent on the quality of the electrode employed. Due to the working gap as low as $G = 5 \mu\text{m}$, the form deviations and occurring burr formation on the electrode have a high impact and are replicated on the workpiece. Besides, the corner radii of the electrodes limit an achievable corner radius of the eroded cavities.

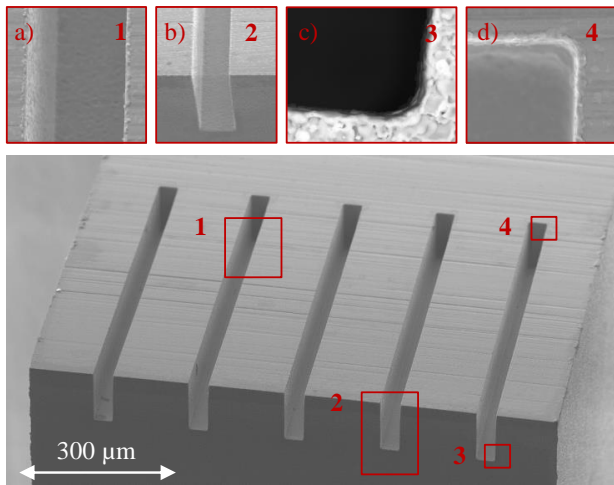


Figure 8 Workpiece eroded using 5 WCu electrodes.

3. Micro-Injection Moulding

Due to the small dimensions and high aspect ratios AR of the micro-cavities in the molds, several factors have to be considered when conducting micro-injection molding. To ensure a high filling ratio R, a premature solicitation of the melt has to be prevented. This can be achieved when pre-heating the mold. The moldability is also determined by the melt volume-flow rate (MVR), melting point θ and type of plastic. For injection-molding two strategies can be applied: isotherm and variotherm. In isotherm the mold is not thermally controlled, whereas in variotherm the mold is heated throughout the process. Also, the air in the mold is evacuated before injection. Molding cavities with an aspect ratio of $AR = 5$ using PMMA using variotherm leads to a filling ratio up to $R = 100 \%$ compared to isotherm with a ratio as low as $R = 30 \%$, as displayed in Figure 9. The variotherm technology is highlighted in red, whereas the isotherm technology is highlighted in blue.

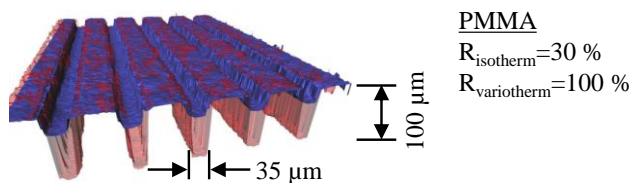


Figure 9 Comparison: isotherm (blue), variotherm (red).

For further examination, the influence of the plastic type is analyzed. Therefore four different thermoplastics are used for micro-injection molding: Polymethyl methacrylate (PMMA), Acrylonitrile-Butadiene-Styrol (ABS), Polyoxymethylene (POM) and Polypropylene (PP). The associated properties are listed in Table 2.

Table 2 Properties of investigated polymers.

	PMMA	ABS	POM	PP
density ρ [g/cm ³]	1.06	1.04	1.2	1.07
@ θ				
melting point θ [°C]	230	220	190	220
expansion coef. α_v [10 ⁻⁶ ·K ⁻¹] @ θ	80	90	110	56
melt volume rate [cm ³ /10min]	3	5.6	12	22.5

The attained width W and height H of the micro-features on the final parts are measured and compared. Doing so allows the determination of the filling ratio of the mold R. Due to different mechanical and physical properties of these materials, the achieved dimensions and thus the filling ratio R differs from the cavity shape, as shown in Figure 10. Three cases are tested: shapes with cavities having widths $W = 60, 35, \text{ and } 35 \mu\text{m}$ and corresponding heights $H = 75, 100, \text{ and } 30 \mu\text{m}$ are machined and used in subsequent micro-injection molding operations. The length is kept constant to $L = 2 \text{ mm}$.

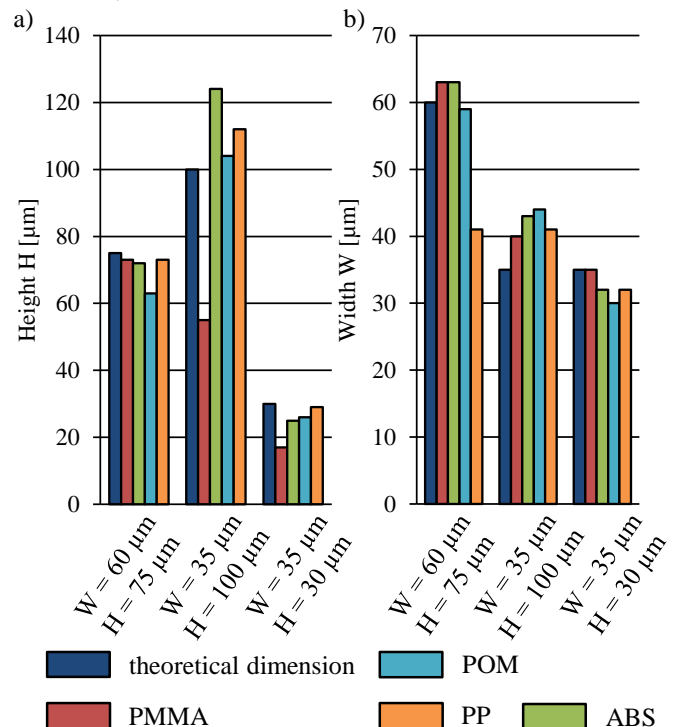


Figure 10 Influence of different plastic types to resultant dimensions of micro-bars when applying variotherm technology; a) achievable height H; b) achievable width W.

According to Figure 10 a), it is feasible to reach a filling ratio in height of $R = 100 \%$ in cavities having an aspect ratio ranging from $AR = 1.25 \dots 3$. ABS and PP reveal the highest potential, as the average filling ratio in height for

the three cases is as high as $\bar{R} = 101\%$ and $\bar{R} = 102\%$. In contrast, the average filling ratio of PMMA merely reaches $\bar{R} = 69\%$. However, the longitudinal filling ratio for ABS is as high as $\bar{R} = 106\%$ and for PP as high as $\bar{R} = 81\%$. The volume filling ratio accumulates for PMMA $\bar{R} = 88\%$, for ABS $\bar{R} = 103\%$, for POM $\bar{R} = 97\%$ and for PP $\bar{R} = 91\%$.

4. Conclusions

The challenges of machining micro-structures are discussed and reliable machining strategies are presented. Injection molding is used for replication of micro-structures, as this technology allows worthy economic machining. However, the shaping of the molds requires a comprehensive preparation and a process chain has to be developed. The mold shaping is conducted using die-sinking EDM, which necessitates structured electrodes made of Cu or WCu. The limitations of each step of the process chain are analyzed and discussed. The dimensions of a final micro-structure are determined by multiple factors, which accumulate throughout the process chain. It was found that micro-milling is the limiting factor in the process chain. The lower limit of a micro-structure is determined primarily by the mechanical properties of the electrode material. The minimal achievable size of a micro-structure and all associated geometrical properties are scaled up during the process by the working gap G during die-sinking EDM. The constraints of each process step are summarized as follows:

- Using micro-milling, flawless and burr-free micro-bars in Cu and WCu are feasible to machine. For both materials, an aspect ratio up to $AR = 6$ can be attained. This corresponds to a width $W_{\text{Bar}} = 50\ \mu\text{m}$ and a height $H_{\text{Bar}} = 290\ \mu\text{m}$. A micro-tool with a diameter of $\varnothing = 150\ \mu\text{m}$ and a cutting edge length $l_{\text{cut}} = 300\ \mu\text{m}$ allows a pitch of $P_{\text{Bar}} = 250\ \mu\text{m}$.
- The quality and form accuracy of the micro-structures determine to a great extent the shape of an eroded cavity. Due to the high flank steepness of the bars, a conicity of $< 2\ \mu\text{m}$ is capable to erode. As the working gap is as low as $G = 5\ \mu\text{m}$, the resultant width of a cavity is as low as $W_{\text{cav}} = 55\ \mu\text{m}$. Inner corner radii of 7 and 3 μm are feasible to achieve when applying two Cu electrodes respectively five WCu electrodes.
- The replication during micro-injection molding is dependent beside other factors on the temperature of the melt and the type of plastic. By applying variotherm technology, a form filling rate of $R = 100\%$ is attainable for micro-structures when using ABS.

5. References

- [1] Annoni, M., Rebaioli, L., Semeraro, Q., 2015, Thin wall geometrical quality improvement in micromilling, *Int J Adv Manuf Technol*, 79/:881–95.
- [2] Benavides, G. L., Bieg, L. F., Saavedra, M. P., Bryce, E. A., 2002, High aspect ratio meso-scale parts enabled by wire micro-EDM, *Microsystem Technologies*, 8/6:395-401.
- [3] Büttner, H., Roth, R., Wegener, K., 2018, Limits of Die-Sinking EDM for micro Structuring in W300 Steel with pure Copper Electrodes, *Procedia CIRP*, 77/:646-9.
- [4] Chen, M., Yao, D., Kim, B., 2001, eliminating flow induced birefringence and minimizing thermally induced residual stresses in injection molded parts, *Polymer-Plastics Technology and Engineering*, 40/4:491-503.
- [5] D'Amore, A., Gabriel, M., Haese, W., Schiff, H., Kaiser, W., 2004, Nano-replication: concentration of information, *Kunststoffe Plast Eur*, 94/:4-7.
- [6] Giboz, J., Copponex, T., Mélé, P., 2007, Microinjection molding of thermoplastic polymers: a review, *Journal of Micromechanics and Microengineering*, 17/6:R96-R109.
- [7] Gillespie, L. K., Blotter, P. T., 1976, The Formation and Properties of Machining Burrs., *Transactions of ASME Journal of Engineers for Industry* 98:66–74.
- [8] Gornik, C., 2004, Injection Moulding of Parts with Microstructured Surfaces for Medical Applications, *Macromolecular Symposia*, 217/1:365-74.
- [9] Hecke, M., Schomburg, W. K., 2003, Review on micro molding of thermoplastic polymers, *Journal of Micromechanics and Microengineering*, 14/3:R1-R14.
- [10] Heisel, U., Klocke, F., Uhlmann, E., Spur, G., 2014, *Handbuch Spanen: Carl Hanser Verlag GmbH & Co. KG*
- [11] Kiswanto, G., Zariatin, D. L., Kob, T. J., 2014, The effect of spindle speed, feed-rate and machining time to the surface roughness and burr formation of Aluminum Alloy 1100 in micro-milling operation, *Journal of Manufacturing Processes*.
- [12] Li, P., Zdebski, D., Langen, H.H., Hoogstrate, A.M., Oosterling, J.A.J., Munnig Schmidt, R.H., Allen, D.M., 2010, Micromilling of thin ribs with high aspect ratios, *J Micromech Microeng*, 20/.
- [13] Llanos, I., Agirre, A., Urreta, H., Thepsonthi, T., Özel, T., 2014, Micromilling high aspect ratio features using tungsten carbide tools, *Proc IMechE Part B: J Engineering Manufacture*:1-9.
- [14] McFarland, A. W., Poggi, M. A., Bottomley, L. A., Colton, J. S., 2005, Injection-moulded scanning force microscopy probes, *Nanotechnology*, 16/8:1249-52.
- [15] Mendoza, R., 2005, Morphologies induites dans les pièces en polyoléfine moulées par injection. Paris: Ecole Nationale Supérieure d'Arts et Métiers.
- [16] Reichenbach, I. G., Bohley, M., Sousa, F. J. P., Aurich, J. C., 2018, Micromachining of PMMA—manufacturing of burr-free structures with single-edge ultra-small micro end mills, *The International Journal of Advanced Manufacturing Technology*, 96/9:3665-77.
- [17] Roy, P., 2001, Micro Plasturgie, *Tech Ing, Plast Compos AM4* 15.
- [18] Schiff, H., David, C., Gabriel, M., Gobrecht, J., Heyderman, L. J., Kaiser, W., et al., 2000, Nanoreplication in polymers using hot embossing and injection molding, *Microelectronic Engineering*, 53/1:171-4.
- [19] Whiteside, B. R., Coates, P. D., Martyn, M. T., In-process monitoring of micromoulding - assessment of process variation.
- [20] Yao, D. G., 2002, Injection molding high aspect ratio microfeatures, *Journal of Injection Molding Technology*, 6/:11-7.
- [21] Zhao, J., Mayes, R. H., Chen, G., Xie, H., Chan, P. S., 2003, Effects of process parameters on the micro molding process, *Polymer Engineering & Science*, 43/9:1542-54.